

ENZYMATIC DEGRADATION OF PLA/CELLULOSE NANOCRYSTAL COMPOSITES

Nóra Hegyesi<sup>1,2,\*</sup>, Yunchong Zhang<sup>3</sup>, Andrea Kohári<sup>1,2</sup>, Péter  
Polyák<sup>1,2</sup>, Xiaofeng Sui<sup>3,\*</sup>, Béla Pukánszky<sup>1,2</sup>

<sup>1</sup>Institute of Materials and Environmental Chemistry, Research  
Centre for Natural Sciences, Hungarian Academy of Sciences, H-  
1519 Budapest, P.O. Box 286, Hungary

<sup>2</sup>Laboratory of Plastics and Rubber Technology, Department of  
Physical Chemistry and Materials Science, Budapest University  
of Technology and Economics, H-1521 Budapest, P.O. Box 91,  
Hungary

<sup>3</sup>Key Lab of Science and Technology of Eco-Textile, Ministry of  
Education, College of Chemistry, Chemical Engineering and  
Biotechnology, Donghua University, Shanghai 201620, People's  
Republic of China

\*Corresponding author: Tel: 36-1-463-2967, E-mail:  
[hegyesi.nora@mail.bme.hu](mailto:hegyesi.nora@mail.bme.hu), [suixf@dhu.edu.cn](mailto:suixf@dhu.edu.cn)

## ABSTRACT

The enzymatic degradation of poly (lactic acid) (PLA) and its nanocomposites reinforced with cellulose nanocrystals (CNC) was catalyzed with lipase from *Candida rugosa* and proteinase K from *Tritirachium album*. The composites were prepared with the Pickering emulsion process and they contained 5, 10 and 15 wt% nanocellulose. Compression molded plates were cut to pieces for the degradation experiments. Preliminary experiments showed that the lipase does not catalyze the degradation of PLA, but the proteinase K is very efficient. The lactic acid forming during the reaction decreases the pH of the degradation medium almost to 4 that leads to the denaturation of the enzyme. Besides pH, the ion concentration of the solution also influences the rate of degradation; smaller ionic strength is more advantageous. The cellulose nanocrystals used for the reinforcement of PLA increase the rate of degradation and the samples disintegrate very rapidly, the polymer degrades in three days. Because the samples lose their integrity, also the amount of lactic acid forming in the process was determined with a colorimetric assay with iron (III) chloride hexahydrate to follow degradation. A model was applied for the quantitative analysis of the kinetics of degradation and denaturation. The rate of both processes doubles in the presence of cellulose nanocrystals. The model and the obtained parameters can be used for the design of experiments and the prediction of the enzymatic degradation of aliphatic polyesters as well as their blends and composites.

KEYWORDS: lipase, protease, buffer solutions, lactic acid, pH, ionic strength, degradation kinetics, denaturation

## 1. INTRODUCTION

Biopolymers are used in increasing amounts in all areas of the economy (Coutinho et al., 2013; Scott, 2018; Miller, 2013). The driving force of the application of these materials is the increased environmental awareness of the industry and the public, depleting resources of fossil energy, increasing difficulties of handling plastic waste, dangerous contamination of natural waters by microplastics, etc. (Imre and Pukánszky, 2013; Ulonska et al., 2018). Biopolymers can be natural polymers like cellulose, starch and lignin or they can be based on natural resources like bio PE or polyamides and also poly(lactic acid) (PLA) (Eerhart et al., 2012; Miller, 2013). Because of its advantageous properties, PLA is used in increasing quantities mostly for packaging and in biomedical applications (Garlotta, 2001). However, PLA has some drawbacks as well, it is very sensitive to water during processing, brittle, crystallizes very slowly, but its physical ageing is relatively fast, which further decreases its fracture resistance. Many attempts are made to overcome these deficiencies by modification.

Various approaches are used to improve the processability and physical properties of PLA. Plasticization and blending improve deformability and impact resistance (Liu and Zhang,

2011; Na et al., 2002), while the use of fillers and reinforcements increases stiffness (Bledzki et al., 2009; Pappu et al., 2019). In order to conserve one of the advantageous properties of PLA, biodegradability, it is often modified with lignocellulosic fibers. The addition of wood and cellulose fibers to PLA increases its stiffness and strength indeed, but decreases deformability even further. An obvious way to overcome this problem is to use cellulosic nanofillers for reinforcement (Zhou et al., 2018). Microfibrillar or bacterial cellulose and cellulose nanocrystals can be added to cellulose in small amounts, still result in considerable improvement of in properties. The stiffness and strength of the polymer increases, amorphous PLA maintains its transparency and even the tendency towards physical ageing may decrease as a result (Müller et al., 2015). In addition, these fillers are also biodegradable (Ling et al., 2018; Szabó and Csiszár, 2017).

PLA is stable under ambient conditions thus its composites reinforced with cellulosic fillers can be used also in structural applications. On the other hand, it is compostable and can be degraded under biological conditions. Composting is a viable way to handle bioplastic waste and produce valuable material as a result. Consequently, the degradation of biopolymers is of theoretical and practical interest, together with the effect of lignocellulosic reinforcements on the degradation process. The degradation of PLA in compost has been studied intensively (Ghorpade et al., 2001). Luzi et al. (Luzi et al., 2015), for

example, investigated the effect of crystalline nanocellulose (CNC) on the compostability of PLA and found that although PLA degraded under the conditions of the compost, the nanocellulose filler did not influence degradation practically at all.

More attempts were made to study the enzymatic degradation of PLA. Enzymes are produced by microorganisms and the same organisms facilitate the degradation of biopolymers in the compost. A wide variety of enzymes was used to accelerate the degradation of PLA including kulinases, lipases, proteases and esterases (Masaki et al., 2005; Pranamuda et al., 2001; Tokiwa and Calabia, 2006; Żen; kiewicz et al., 2013; Rytlewski et al., 2018). The various enzymes catalyzed the degradation of PLA in different extents depending on the conditions of degradation. Certain lipases are advantageous because of their larger resistance against environmental effects including solvents (Doukyu and Ogino, 2010; Ogino et al., 1994). Although quite a few of the enzymes catalyzed the degradation of PLA in smaller or larger extent, proteinase seemed to be the most efficient among the enzymes used up to now.

The effect of lignocelulosic reinforcements on the enzymatic degradation of PLA was also investigated in a few cases. Stepczynska and Rytlewski (Stepczyńska and Rytlewski, 2018) studied the enzymatic degradation of PLA reinforced with flax and found that weight decrease is larger in its presence than without it and explained the phenomenon with the formation of channels due to the presence of the fibers. On the other hand,

Luzi et al. (Luzi et al., 2015) found that the degradation of PLA slowed down considerably in the presence of crystalline nanocellulose already at 1 wt% filler content. They also followed degradation by the determination of the weight loss of the samples.

Because of the importance of the biodegradation of PLA reinforced with cellulose nanocrystal fillers and due to the contradictory nature of the conclusions published, the goal of this work was to study the enzymatic degradation of PLA modified with crystalline nanocellulose. Two different enzymes were employed and degradation was followed not only by the measurement of weight, but also by an analytical technique. The influence of various factors on the enzymatic degradation of PLA was studied including the effect of the degradation product and ion concentration. The kinetics of degradation was analyzed quantitatively with the help of an appropriate model. Importance for practice is also mentioned in the final section of the paper.

## 2. EXPERIMENTAL

### 2.1. Materials

The PLA used in the experiments was the Ingeo 2003D grade supplied by Natureworks, USA with a D-lactic acid content of 1.4%, density of 1.24 g/cm<sup>3</sup>, number-average molecular weight ( $M_n$ ) of 150,000 Da and polydispersity of 1.33. Wood pulp was obtained from Xinxiang Natural Chemical Co., Ltd. The viscosity-average degree of polymerization was estimated to be 870 according to

measurements using an Ubbelohde viscometer in cupric ethylene diamine hydroxide solution (CUEN). The lipase from *Candida rugosa* (CRL) was purchased from Sigma Aldrich, while the proteinase K from *Tritirachium album* was supplied by VWR International. The activity of the first was 15-25, while that of the second 40 U/mg. Dichloromethane (DCM) (Molar Chemicals, 99 %), Milli-Q distilled water (Millipore,  $\rho > 18.2 \text{ M}\Omega\text{cm}$ ), sodium phosphate (Alpha Asear, 97 %), sodium chloride (Molar Chemicals, 99.97 %), tris(hydroxymethyl) aminomethane (Molar Chemicals, 99.5 %) (Tris), ortho-phosphoric acid (Molar Chemicals 85.44 %), hydrochloric acid (Molar Chemicals, 36.67 %), lactic acid (VWR International, 1.0 N aqueous solution) and iron (III) chloride hexahydrate (Riedel-de Haen, min 99 %) were used as received.

## **2.2. Preparation of the buffer solutions**

Various buffer solutions were prepared with different pH (7.2 and 8.6) and ionic strength ( $I = 12, 25, \text{ and } 100 \text{ mM}$ ) values. In the case of the phosphate buffer (PBS) (pH = 7.2), 30 mmol (4.9182 g)  $\text{Na}_3\text{PO}_4$  was dissolved in Milli-Q water and 20 mmol (2.3059 g,  $1.28 \text{ cm}^3$ )  $\text{o-H}_3\text{PO}_4$  was added. The exact pH of the buffer was adjusted with the addition of HCl. The solution was placed into a measuring flask of 1 l volume; it was filled up to sign and homogenized.

Buffers of pH = 8.6 were prepared with dissolving 50 mmol (6.057 g) ( $I = 12 \text{ mM}, c = 50 \text{ mM}$ ) or 100 mmol (12.114 g) ( $I = 25$

mM,  $c = 100$  mM) Tris in 900 ml MilliQ water and the pH of the solution was adjusted with the addition of HCl, finally the solutions were diluted to 1 l in a measuring flask. The third tris buffer ( $I = 100$  mM,  $c = 100$  mM) was prepared with same method as the buffer with  $I = 25$  mM just 7.3 mmol (0.427 g) NaCl was added to increase the ionic strength without changing buffer concentration.

### **2.3. Preparation of cellulose nanocrystals**

Hydrochloric acid was poured into a desiccator. The valve of the desiccator was left open for a day for HCl to fill the vessel completely. Wood pulp was placed into the desiccator next and left standing for 8 hours. Excessive HCl was washed from the pulp afterwards, and then the pulp was subjected to ultrasonic treatment and high-pressure homogenization. The product was re-dispersed with sonication for 10 min. The cellulose content of the obtained dispersion was 1.01 wt%. The particles obtained are typically rigid rod-shaped monocrystalline cellulose domains with about 15 nm in diameter and 360 nm in length. (Zhang et al., 2019).

### **2.4. Preparation of PLA/CNC nanocomposites**

The dispersion of cellulose nanocrystals was diluted with deionized water to achieve concentrations of 0.25, 0.5 and 0.75 w/v%. A PLA solution of 100 mg/ml concentration was prepared in dichloromethane. 10 ml of this solution was added to the CNC



suspension and then the emulsion obtained was stirred at 12000 rpm for 3 min and then sonicated for 3 min. Dichloromethane was evaporated from the system at ambient temperature in 24 hours. The remaining material was filtered with a 500 mesh vacuum filter. The obtained filtrate was dried under vacuum at 60 °C for 24 hours. The composite powder was compression molded into plates at 180 °C and 5 min. The composites contained 5, 10 and 15 wt% CNC, respectively.

## **2.5. Methods and characterization**

The pH of the buffers was determined using a Metrohm 827 type apparatus with combined glass electrode. The crystalline structure of the PLA/CNC nanocomposites was characterized by X-ray diffraction measurements using a Phillips PW 1830 equipment with  $\text{CuK}\alpha$  irradiation at 40 KV and 35 mA anode excitation between 5 and 40°  $2\theta$  angles with 0.04°/step scan rate. The structure of the composites and that of the degraded samples was characterized by scanning electron microscopy (SEM) using a Jeol JSM 6380 apparatus. Micrographs were recorded after sputter coating with gold on fracture surfaces created at ambient temperature.

## **2.6. Degradation studies**

The compression molded plates of neat PLA and the composites were cut to pieces of 15 x 15 mm dimensions. The samples were placed into vials and the enzyme solution or the buffer (reference) was measured onto the specimens. The vials were

shaken at 200 rpm and 37 °C afterwards. Three parallel measurements were done during the preliminary experiments, while individual samples were investigated in the other cases. In the preliminary experiments, the pieces were taken from the vial at certain time intervals, washed with water, wiped, weighed, and then re-immersed into the same solution. In the other experiments, the samples were taken from the vial after a certain time, washed with water, wiped, dried in a vacuum oven at 25 °C and 200 mbar for 12 h and weighed. The concentration of the enzyme was selected according to literature references (Dogan et al., 2017; Stepczyńska and Rytlewski, 2018; Żenkiewicz et al., 2013).

Besides the measurement of weight loss, degradation was followed also by the determination of the main degradation product, lactic acid. The monomer forms a complex with iron(III) chloride hexahydrate which has an adsorption maximum at 390 nm in the UV-Vis spectrum (Borshchevskaya et al., 2016). 3 ml reagent solution (3 mg/ml) was added to 75 µl degradation medium to form the complex. Background was recorded with 3 ml reagent and 75 µl buffer. Spectra were recorded using a Unicam UV-500 apparatus between 190 and 600 nm at 600 nm/min scan rate and 1 nm resolution in a quartz cuvette of 1 cm thickness.

### 3. RESULTS AND DISCUSSION

The results are discussed in several sections. Those of the preliminary experiments directed towards the selection of the

proper enzyme are presented first, and then the effect of experimental conditions on the extent and rate of degradation are shown next. The degradation of the nanocomposites and the effect of the nanofiller on it are discussed in the subsequent section followed by the quantitative analysis of degradation kinetics.

### **3.1. Preliminary experiments**

The goal of the preliminary experiments was to select the enzyme used in the further course of the study. Based on literature information, we selected the lipase from *Candida rugosa* (CRL) and a protease (proteinase K from *Tritirachium album*). Lipases are very robust and are not sensitive to environmental conditions (Doukyu and Ogino, 2010; Ogino et al., 1994), and several reports indicated their smaller or larger efficiency in the degradation of various aliphatic polyesters (F Williams, 1981; Gan et al., 1999; Lee et al., 2014; Malwela and Ray, 2015; Nakajima-Kambe et al., 2012). On the other hand, quite a number of studies indicated that proteinase K degrades PLA efficiently (Dogan et al., 2017; Luzi et al., 2015; Stepczyńska and Rytlewski, 2018; Żenkiewicz et al., 2013). The relative weight loss observed in the presence of CRL is plotted in **Fig. 1** as a function of time. The total weight loss at equilibrium is around 1.5 % and the decrease of weight measured in the buffer not containing the enzyme is only slightly smaller. The presence of lactic acid was checked in the degradation solution by the

analytical technique described in the experimental part and we could not detect any monomer in the solution at all. We had to draw the conclusion from these results that CRL does not catalyze the degradation of our PLA.

<Fig. 1>

Weight loss of neat PLA in the presence of CRL. Symbols: (○) with enzyme, (□) buffer (pH = 7.2).

Similar experiments were carried out with proteinase K as well. The samples lost much more weight quite fast, but degradation stopped in a relatively short time. Degradation restarted after changing the degradation medium, but it stopped again very soon (**Fig. 2**). The measurement of the pH of the solution showed that pH changed from the original value of 8.6 to around 4.3-4.5. According to the producer the optimum pH range of this enzyme is between 6.5 and 12, thus we must assume that the drastic decrease of pH resulted in the denaturation of the enzyme. We must call the attention here also to the weight measured in the buffer itself. Weight decreased only about 1.3 % at pH 7.2, while weight loss was approximately 5 % at 8.6. Probably the hydroxide ions present at pH 8.6 catalyzed the hydrolytic degradation of PLA in accordance with the findings of Tsuji and Ikarashi (Tsuji and Ikarashi, 2004). According to the results of the preliminary study, we decided to conduct further experiments with proteinase K, but the results also called

attention to the role of the degradation product and the importance of pH during degradation.

<Fig. 2>

Catalytic action of proteinase K in the degradation of neat PLA. Effect of pH and the exchange of the degradation medium. Symbols: (○) with enzyme, (□) buffer (pH = 8.6, I = 12 mM).

### 3.2. Effect of pH

The preliminary experiment carried out with proteinase K indicated that the pH of the degradation medium changes with time and degradation stops, probably because of the denaturation of the enzyme. Consequently, the change of pH was followed as a function of time in another experiment. According to [Fig. 3](#) pH decreases continuously indeed, practically linearly at the beginning and then slowing down at longer times. Weight loss is plotted in the figure as well for comparison. The two correlations correspond to each other perfectly, weight loss increases proportionally with time first and then it slows down and stops at longer times. Obviously, the formation of the degradation product, lactic acid (pKa = 3.86), changes pH and stops the degradation of the polymer.

<Fig. 3>

Effect of pH on the degradation (weight loss) of neat PLA. Decreasing rate below pH = 6.5. Symbols: (○) weight loss, (□)

pH. (initial pH = 8.6, I = 12 mM)

The analysis of the data showed that degradation slows down at around 33 % weight loss resulting in 27 mmol/l lactic acid concentration. At this concentration, the buffer capacity of the solution is exhausted, pH decreases below a critical value, around 6.5, at which the enzyme is not active any more. The denaturation of the enzyme leads to the slow down and stopping of degradation. This observation is in close agreement with that of Ghorpade et al. (Ghorpade et al., 2001) who found that a compost could not contain more than 30 wt% PLA without losing its capacity to degrade the polymer. They explained the phenomenon with the formation of excessive lactic acid, which decreased pH and destroyed microorganisms. The results presented in this section showed that further experiments must be carried out in buffers with larger capacity.

### **3.3. Ion concentration**

The effect of the ionic strength of the degradation medium was investigated in a further experiment. The measurements were carried out with the neat PLA, but also with the nanocomposites. The effect of ion concentration on the weight loss of the neat polymer is presented in [Fig. 4](#). Weight did not change in the buffer at all, but considerable weight loss was measured in the two solutions with different ionic strengths. With increasing ion concentration, the weight loss reached in equilibrium

decreased considerably indicating that larger ion concentration decreases the activity of the enzyme. As a result of these measurements, the decision was made to continue experiments with a buffer of smaller ionic strength.

<Fig. 4>

Influence of the ionic strength of the buffer solution on the activity of proteinase K. Symbols: ( $\Delta$ ) enzyme, I = 25 mM, (O) enzyme, I = 100 mM, ( $\square$ ) buffer, I = 100 mM (pH = 8.6).

### **3.4. Enzymatic degradation**

Degradation was followed in different ways. Changes in the morphology and structure of the specimens gave some qualitative information about degradation, while the measurement of weight loss and the analytical method used yielded quantitative results.

#### *3.4.1. Structure*

Photos were taken of the specimens after sampling to follow changes in morphology. They are presented in [Fig. 5](#). The neat PLA became opaque after a day, then its smooth edges changed to sharp and broken ones, later the pieces became thinner and holes appeared in them. Finally, also the shape of the originally rectangular specimens changed and became irregular. Nevertheless, the specimens could be handled, weighed and photographed for a relatively long time. PLA containing the

nanocellulose reinforcement, on the other hand, behaved completely differently. The samples fell apart very fast and disintegrated within a few days. This made impossible the measurement of their weight, thus the following of degradation in the usual way.

<Fig. 5>

Changes in the appearance of neat PLA and disintegration of the PLA/CNC composites during their enzymatic degradation (pH = 8.6, I = 25 mM).

The structure of the degraded samples was checked also by scanning electron microscopy. SEM micrographs recorded on a specimen containing 15 wt% crystalline nanocellulose before the start of the degradation experiment and after degradation for two days are shown in **Fig. 6**. Clusters of the reinforcement can be clearly seen in the micrograph indicating that the degradation and disappearance of the PLA matrix might leave a more porous surface behind.

<Fig. 6>

SEM micrographs recorded on the fracture surface of the neat PLA/CNC nanocomposite containing 15 wt% CNC and on the same surface after 48 hours of enzymatic degradation (pH = 8.6, I = 25 mM), respectively.



Further information is offered about the structure of the composites by XRD measurements. Traces of PLA and its composites before and after 48 hour degradation are presented in **Fig. 7**. The broad peak between  $9$  and  $27^\circ$  of the neat PLA shows that the polymer is practically completely amorphous which also can be observed on the diffractograms of the composites. This fact explains the fast degradation, since crystalline PLA degrades much slower (Tsuji and Ikarashi, 2004). The XRD traces of the composites differ considerably from that of the neat PLA. The peaks characteristic for crystalline cellulose appear clearly in the trace and superimpose onto the amorphous halo of PLA (**Fig 7a**). The intensity of the reflections at  $16.5$  and  $22.7^\circ$  increases with increasing nanocellulose content. These reflections become even more pronounced after degradation, and they dominate the diffractogram (**Fig. 7b**). Obviously, PLA degrades and it is removed from the composite leaving behind the cellulose nanocrystals. All these results prove that enzyme solutions degrade PLA indeed and nanocellulose facilitates degradation. It also indicates that CNC remains intact during the process.

<Fig. 7>

XRD traces of neat PLA and that of the CNC nanocomposites a) before the degradation experiment and b) after 48 h degradation (pH = 8.6, I = 25 mM) (b).

### 3.4.2. Weight loss

The enzymatic degradation of aliphatic polyesters is usually followed by the measurement of weight, the determination of weight loss. The results of such measurements are presented in **Fig. 8** for the neat PLA and the PLA/CNC composites. In accordance with the results shown in **Fig. 5**, degradation could be followed with this method quite well in the case of the neat polymer, but not for the composites, since they disintegrated very rapidly within a few days. The correlation obtained for the neat polymer is in complete agreement with previous results, after a certain time degradation slows down and converges towards a constant value, which however is very close to 100 %. The few results obtained for the composites indicate that weight loss is inversely proportional to nanocellulose content, i.e. the weight loss measured became smaller with increasing CNC content. These results and those presented in the previous section completely justify the use of another method for the detection of the degradation of the polymer.

<Fig. 8>

Relative weight loss of PLA samples measured during their enzymatic degradation in the presence of the proteinase K.  
Symbols: (□) neat PLA, (○) 5, (△) 10, (▽) 15 wt% crystalline nanocellulose (pH = 8.6, I = 25 mM).

### 3.4.3. Quantitative analysis of the degradation product

Since composite samples disintegrated after a relatively short time, the usual technique of measuring weight loss could not be used to follow degradation. On the other hand, the determination of the amount of degradation product, lactic acid, proved to be an adequate method for this purpose. The formed lactic acid could be recalculated into weight loss after calibration ( $\epsilon_{390 \text{ nm}} = 17.611 \text{ dm}^3\text{mol}^{-1}\text{cm}^{-1}$ ), and this calculated weight loss is plotted against degradation time in **Fig. 9**. Only two correlations are drawn in the figure to avoid confusion, but all the measured points are plotted. The results indicate that cellulose nanocrystals accelerate degradation compared to the neat polymer. However, large CNC content results in smaller degree of degradation, the reaction stops earlier than in the case of the neat polymer. The results clearly indicate that complexation using iron(III) chloride hexahydrate is an adequate method for the following of the enzymatic degradation of PLA.

<Fig. 9>

Relative weight loss calculated from the results of UV-Vis measurements plotted against the time of enzymatic degradation. Symbols are the same as in **Fig. 8**.

Because of the acidic character of the degradation product and the effect of pH on the degradation process, pH was monitored in all series of measurements done. The purpose of the

determination was to see, if excessive denaturation of the enzyme occurred, or any other effect influenced pH and the rate as well as the extent of degradation. In [Fig. 10](#), the pH of the degradation medium is plotted against the amount of lactic acid formed in the experiments for the neat PLA and the three nanocomposites (see [Fig. 9](#)). pH decreases slowly and almost proportionally up to a certain lactic acid concentration and then decreases very steeply. The sudden and steep change indicates that besides the formation of lactic acid another factor might also influence the kinetics of degradation. This factor is the loss of the capacity of the Tris buffer at this pH (Persat et al., 2009), and thus the formation of a small amount of lactic acid leads to the sharp decrease of the pH of the solution. This calls attention again to the importance of choosing the proper medium for degradation.

<Fig. 10>

pH of the degradation solution plotted against its lactic acid concentration. Non-linear correlation due to changing buffer capacity. Symbols are the same as in [Fig. 8](#).

### **3.5. Degradation kinetics**

In order to analyze degradation properly and see the effect of cellulose nanocrystals on its rate, a model is needed which describes degradation kinetics quantitatively. The most frequently used model for the description of the kinetics of

enzymatic reactions was proposed by Michaelis and Menten (Michaelis and Menten, 1913). Unfortunately, the model was developed for homogeneous reactions, and usually it is used only for the description of experiments carried out for a short time, in the linear section of the reaction (Polyák et al., 2018). In our case, the reaction is heterogeneous, and degradation is carried out for a long time, for days compared to several hundred minutes. Under such conditions, enzymatic degradation proceeds in three steps. The first step of the process is the adsorption of the enzyme on the surface of the substrate. This is followed by the degradation of the polymer, which may be described by the original Michaelis-Menten approach. Finally, after longer times, the denaturation of the enzyme may take place and the reaction slows down, just as in our case (see [Figs. 2, 4, 8 and 9](#)).

The model, which describes the kinetics of enzymatic degradation quantitatively, must consider all three steps. However, since the adsorption of the enzyme on the substrate takes place first and in a short time compared to the entire length of the measurement, we ignore it here in order to simplify treatment. If we follow degradation by the loss of sample weight, the rate of degradation in the linear stage, as predicted by the Michaelis-Menten model (Michaelis and Menten, 1913), can be described with the following differential equation

$$\frac{dm(t)}{dt} = v_d \quad (1)$$

where  $v_d$  is the rate of degradation,  $m$  the weight loss of the

sample and  $t$  time. However, we must take into account the denaturation of the enzyme, which results in the decrease of degradation rate. If we assume that denaturation proceeds according to first order kinetics, the rate of mass loss can be expressed as

$$\frac{dm(t)}{dt} = v_d - \frac{m(t)}{\tau} \quad (2)$$

where  $\tau$  is the time constant of denaturation, which expresses the rate of the loss of activity of the enzyme. After the necessary operations and integration we obtain the following solution

$$m(t) = C \exp(-t/\tau) + v_d \tau \quad (3)$$

where  $C$  is an integration constant the value of which can be determined from the initial conditions of the setup. After defining  $C$  and rearrangement, we come to the final solution

$$m(t) = v_d \tau [1 - \exp(-t/\tau)] \quad (4)$$

The three parameters of [Eq. 4](#) all have real physical meaning.  $v_d$  gives the initial rate of degradation at zero time,  $\tau$  is a time constant which is related to the rate of denaturation, and the pre-exponential term  $A = v_d \tau$  equals the loss of mass at infinite time, i.e. the amount of polymer degraded by the enzyme. Naturally, the model can be used not only for the analysis of mass loss, but also any other quantity characterizing the degradation of aliphatic polyesters, i.e. the absorbance of the

complex formed from the reaction of lactic acid and iron(III) chloride hexahydrate.

The model can be verified by fitting **Eq. 4** to the experimental results. The solid lines in **Figs. 2** and **9** are fitted correlations and describe the results very well. Fitting the model to the experimental values allows the determination of the constants, which characterize the rate of degradation and denaturation. The calculations have been carried out for all the experiments done in the project as a function of time, but we present only the most important results here to support our conclusions. The parameters obtained for the two-step correlation of **Fig. 2** and those presented in **Fig. 9** are collected in **Table 1**.

The results listed in **Table 1** show that in spite of the fact that the composition of the initial degradation solution and that used in the second step was exactly the same, the degradation is much faster in the second stage than in the first. A possible reason for this increase might be the changing of the surface roughness of samples, which degraded to a certain extent. Roughness increases the available surface of the specimen (see **Fig. 6**). Since degradation proceeds on the surface, its rate increases as a result. Similarly, the rate of denaturation also increases, but this is probably the consequence of increased degradation rate. Faster degradation results in more lactic acid, faster change of pH and earlier denaturation. The parameters obtained for the neat PLA and the three composites

are listed in the last four rows of **Table 1**. Apart from the composite containing 5 wt% nanocellulose, the rate of degradation increases considerably in the presence of the reinforcement (see **Fig. 11**). Such an increase was observed by Stepczynska and Rytlewski (Stepczyńska and Rytlewski, 2018) and they explained it with the formation of some kind of channels, which conduct water into the polymer. However, degradation occurs only on the surface of the samples, since enzyme molecules are large and cannot diffuse into the polymer. We believe instead that degradation removes PLA leading to the disintegration of the samples and larger surface area, which allows the enzyme to adsorb on the surface and accelerate degradation. Besides the rate of degradation, also the time constant of denaturation is plotted in **Fig. 11** as a function of nanocellulose content. The rate of denaturation also increases, partly because of the faster rate of degradation (see above), but also because of the exhaustion of the buffer. Kinetic analysis verified our qualitative conclusions drawn from the results and expressed the effect of various factors quantitatively. The rate of denaturation has especially large importance, because it determines the lifetime of the degradation medium, the time until the enzyme used as catalyst is active.

<Fig.11>

Effect of CNC content on the rate of degradation and the time constant of denaturation during the enzymatic degradation of



PLA/CNC nanocomposites. Symbols: (○) rate of degradation,  $v_d$ ;

(□) time constant of denaturation,  $\tau$  (see [Eq. 1](#)).

#### 4. CONCLUSIONS

Preliminary experiments showed that the lipase from *Candida rugosa* does not catalyze the degradation of PLA, but proteinase K is very efficient. The lactic acid forming during the reaction is a relatively strong acid, changes the pH of the degradation medium that leads to the denaturation of the enzyme. Denaturation occurs below pH = 6.5, thus either the degradation solution must be changed regularly or a buffer with sufficient capacity must be used as medium. Besides pH, the ion concentration of the solution also influences the rate of degradation; smaller ionic strength is more advantageous. The cellulose nanocrystals used for the reinforcement of PLA increase the rate of degradation and the samples disintegrate very rapidly. Because the samples lose their integrity, an alternative method is needed to follow degradation. This can be done by the determination of the amount of lactic acid forming during degradation. Complex formation with iron(III) chloride hexahydrate and UV-Vis spectroscopy proved to be a very appropriate method for the purpose. A model was applied for the quantitative analysis of the kinetics of degradation and denaturation, which takes into account and describes both processes well. The model and the obtained parameters can be used for the design of experiments and the prediction of the degradation of aliphatic polyesters as well as their blends and composites.

## 5. ACKNOWLEDGEMENTS

The National Research Fund of Hungary (OTKA K 120039) and the BME-Nanonotechnology FIKP grant of EMMI (BME FIKP-NAT) are greatly acknowledged for the financial support of this research. The authors are indebted to András Bartos for the SEM micrographs as well as Muriel Józó and Vilmos Lóvi for lactic acid calibration.

## 6. REFERENCES

- Bledzki, A.K., Jaszkievicz, A., Scherzer, D., 2009. Mechanical properties of PLA composites with man-made cellulose and abaca fibres. *Composites Part A* 40, 404-412.
- Borshchevskaya, L.N., Gordeeva, T.L., Kalinina, A.N., Sineokii, S.P., 2016. Spectrophotometric determination of lactic acid. *J. Anal. Chem.* 71, 755-758.
- Coutinho, P.L.d.A., Morita, A.T., Cassinelli, L.F., Morschbacker, A., Carmo, R.W.D., 2013. Braskem's Ethanol to Polyethylene Process Development, Catalytic Process Development for Renewable Materials, pp. 149-165.
- Dogan, S.K., Boyacioglu, S., Kodal, M., Gokce, O., Ozkoc, G., 2017. Thermally induced shape memory behavior, enzymatic degradation and biocompatibility of PLA/TPU blends: "Effects of compatibilization". *J Mech Behav Biomed Mater* 71, 349-361.
- Doukyu, N., Ogino, H., 2010. Organic solvent-tolerant enzymes. *Biochem. Eng. J.* 48, 270-282.

Eerhart, A.J.J.E., Faaij, A.P.C., Patel, M.K., 2012. Replacing fossil based PET with biobased PEF; process analysis, energy and GHG balance. *Energ Environ Sci* 5, 6407-6422.

F Williams, D., 1981. *Enzymic Hydrolysis of Polylactic Acid*.

Gan, Z., Yu, D., Zhong, Z., Liang, Q., Jing, X., 1999. Enzymatic degradation of poly( $\epsilon$ -caprolactone)/poly(dl-lactide) blends in phosphate buffer solution. *Polymer* 40, 2859-2862.

Garlotta, D., 2001. A Literature Review of Poly(Lactic Acid). *J. Polym. Environ.* 9, 63-84.

Ghorpade, V.M., Gennadios, A., Hanna, M.A., 2001. Laboratory composting of extruded poly(lactic acid) sheets. *Bioresour. Technol.* 76, 57-61.

Imre, B., Pukánszky, B., 2013. Compatibilization in bio-based and biodegradable polymer blends. *Eur. Polym. J.* 49, 1215-1233.

Lee, S.H., Kim, I.Y., Song, W.S., 2014. Biodegradation of polylactic acid (PLA) fibers using different enzymes. *Macromol. Res.* 22, 657-663.

Ling, Z., Zhang, X., Yang, G., Takabe, K., Xu, F., 2018. Nanocrystals of cellulose allomorphs have different adsorption of cellulase and subsequent degradation. *Ind. Crop. Prod.* 112, 541-549.

Liu, H., Zhang, J., 2011. Research progress in toughening modification of poly(lactic acid). *J. Polym. Sci., Part B: Polym. Phys.* 49, 1051-1083.

Luzi, F., Fortunati, E., Puglia, D., Petrucci, R., Kenny, J.M., Torre, L., 2015. Study of disintegrability in compost and

enzymatic degradation of PLA and PLA nanocomposites reinforced with cellulose nanocrystals extracted from *Posidonia Oceanica*. *Polym. Degrad. Stab.* 121, 105-115.

Malwela, T., Ray, S.S., 2015. Enzymatic degradation behavior of nanoclay reinforced biodegradable PLA/PBSA blend composites. *Int. J. Biol. Macromol.* 77, 131-142.

Masaki, K., Kamini, N.R., Ikeda, H., Iefuji, H., 2005. Cutinase-Like Enzyme from the Yeast *Cryptococcus* sp. Strain S-2 Hydrolyzes Polylactic Acid and Other Biodegradable Plastics. *Appl. Environ. Microbiol.* 71, 7548-7550.

Michaelis, L., Menten, M., 1913. Die Kinetik der Invertinwirkung. *Biochem. Z.* 49, 333-369.

Miller, S.A., 2013. Sustainable Polymers: Opportunities for the Next Decade. *ACS Macro Lett.* 2, 550-554.

Müller, P., Imre, B., Bere, J., Móczó, J., Pukánszky, B., 2015. Physical ageing and molecular mobility in PLA blends and composites. *J. Therm. Anal. Calorim.* 122, 1423-1433.

Na, Y.-H., He, Y., Shuai, X., Kikkawa, Y., Doi, Y., Inoue, Y., 2002. Compatibilization Effect of Poly( $\epsilon$ -caprolactone)-*b*-poly(ethylene glycol) Block Copolymers and Phase Morphology Analysis in Immiscible Poly(lactide)/Poly( $\epsilon$ -caprolactone) Blends. *Biomacromolecules* 3, 1179-1186.

Nakajima-Kambe, T., Edwinoliver, N.G., Maeda, H., Thirunavukarasu, K., Gowthaman, M.K., Masaki, K., Mahalingam, S., Kamini, N.R., 2012. Purification, cloning and expression of

an *Aspergillus niger* lipase for degradation of poly(lactic acid) and poly( $\epsilon$ -caprolactone). *Polym. Degrad. Stab.* 97, 139-144.

Ogino, H., Miyamoto, K., Ishikawa, H., 1994. Organic-Solvent-Tolerant Bacterium Which Secretes Organic-Solvent-Stable Lipolytic Enzyme. *Appl. Environ. Microbiol.* 60, 3884-3886.

Pappu, A., Pickering, K.L., Thakur, V.K., 2019. Manufacturing and characterization of sustainable hybrid composites using sisal and hemp fibres as reinforcement of poly (lactic acid) via injection moulding. *Ind. Crop. Prod.* 137, 260-269.

Persat, A., Chambers, R.D., Santiago, J.G., 2009. Basic principles of electrolyte chemistry for microfluidic electrokinetics. Part I: Acid-base equilibria and pH buffers. *Lab Chip* 9, 2437-2453.

Polyák, P., Dohovits, E., Nagy, G.N., Vértessy, B.G., Vörös, G., Pukánszky, B., 2018. Enzymatic degradation of poly-[(R)-3-hydroxybutyrate]: Mechanism, kinetics, consequences. *Int. J. Biol. Macromol.* 112, 156-162.

Pranamuda, H., Tsuchii, A., Tokiwa, Y., 2001. Poly (L-lactide)-Degrading Enzyme Produced by *Amycolatopsis* sp. *Macromol. Biosci.* 1, 25-29.

Rytlewski, P., Stepczyńska, M., Gohs, U., Malinowski, R., Budner, B., Żenkiewicz, M., 2018. Flax fibres reinforced polylactide modified by ionizing radiation. *Ind. Crop. Prod.* 112, 716-723.

Scott, A., 2018. Lego plants to be made from plants. *C&EN Global Enterprise* 96, 16-16.

Stepczyńska, M., Rytlewski, P., 2018. Enzymatic degradation of flax-fibers reinforced polylactide. *Int. Biodeterior. Biodegrad.* 126, 160-166.

Szabo, O.E., Csiszar, E., 2017. Some factors affecting efficiency of the ultrasound-aided enzymatic hydrolysis of cotton cellulose. *Carbohydr. Polym.* 156, 357-363.

Tokiwa, Y., Calabria, B.P., 2006. Biodegradability and biodegradation of poly(lactide). *Appl. Microbiol. Biotechnol.* 72, 244-251.

Tsuji, H., Ikarashi, K., 2004. In vitro hydrolysis of poly(l-lactide) crystalline residues as extended-chain crystallites: III. Effects of pH and enzyme. *Polym. Degrad. Stab.* 85, 647-656.

Ulonska, K., König, A., Klatt, M., Mitsos, A., Viell, J., 2018. Optimization of Multiproduct Biorefinery Processes under Consideration of Biomass Supply Chain Management and Market Developments. *Ind. Eng. Chem. Res.* 57, 6980-6991.

Żenkiewicz, M., Richert, A., Malinowski, R., Moraczewski, K., 2013. A comparative analysis of mass losses of some aliphatic polyesters upon enzymatic degradation. *Polym. Test.* 32, 209-214.

Zhang, Y., Cui, L., Xu, H., Feng, X., Wang, B., Pukánszky, B., Mao, Z., Sui, X., 2019. Poly(lactic acid)/cellulose nanocrystal composites via the Pickering emulsion approach: Rheological, thermal and mechanical properties. *Int. J. Biol. Macromol.* 137, 197-204.

Zhou, L., He, H., Li, M.-c., Huang, S., Mei, C., Wu, Q., 2018. Enhancing mechanical properties of poly(lactic acid) through its

in-situ crosslinking with maleic anhydride-modified cellulose nanocrystals from cottonseed hulls. *Ind. Crop. Prod.* 112, 449-459.

Table 1 Kinetic parameters of the degradation of PLA and its nanocomposites as well as the denaturation of the enzyme (see [Eq. 1](#))

Experiment	CNC content (wt%)	$v_d$ (%/h)	$\tau$ (h)	A (%)
preliminary	0	0.51	32.7	16.8
	0	2.31	11.9	27.5
degradation	0	1.01	97.6	98.6
	5	0.95	95.5	90.7
	10	1.89	46.2	87.1
	15	1.96	41.4	81.1



## CAPTIONS

- Fig. 1 Weight loss of neat PLA in the presence of CRL. Symbols: (O) with enzyme, (□) buffer (pH = 7.2).
- Fig. 2 Catalytic action of proteinase K in the degradation of neat PLA. Effect of pH and the changing of the degradation medium. Symbols: (O) with enzyme, (□) buffer (pH = 8.6, I = 12 mM).
- Fig. 3 Effect of pH on the degradation (weight loss) of neat PLA. Decreasing rate below pH = 6.5. Symbols: (O) weight loss, (□) pH. (initial pH = 8.6, I = 12 mM)
- Fig. 4 Influence of the ionic strength of the buffer solution on the enzymatic activity of proteinase K. Symbols: (Δ) enzyme, I = 25 mM, (O) enzyme, I = 100 mM, (□) buffer, I = 100 mM (pH = 8.6).
- Fig. 5 Changes in the appearance of neat PLA and disintegration of the PLA/CNC composites during their enzymatic degradation (pH = 8.6, I = 25 mM).
- Fig. 6 SEM micrographs recorded on the fracture surface of the PLA/CNC nanocomposite containing 15 wt% CNC a) before degradation and b) after 48 hours of enzymatic degradation (pH = 8.6, I = 25 mM).
- Fig. 7 XRD traces of neat PLA and that of the CNC nanocomposites a) before the start of the degradation experiments and b) after 48 h degradation (pH = 8.6, I = 25 mM).
- Fig. 8 Relative weight loss of PLA samples measured during

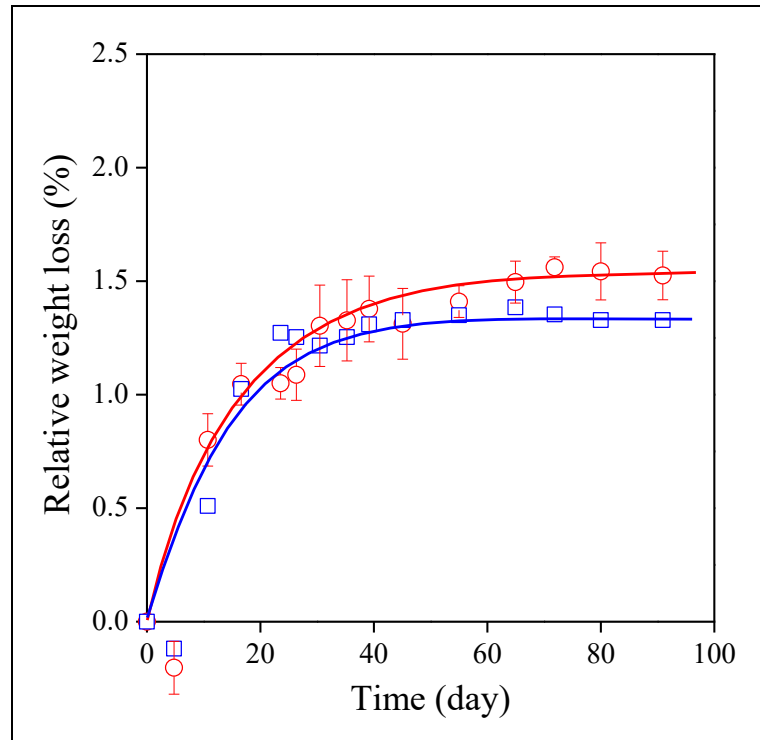
their enzymatic degradation in the presence of ~~the~~ proteinase K. Symbols: ( $\square$ ) neat PLA, ( $\circ$ ) 5, ( $\triangle$ ) 10, ( $\nabla$ ) 15 wt% crystalline nanocellulose (pH = 8.6, I = 25 mM).

Fig. 9 Relative weight loss calculated from the results of UV-Vis measurements plotted against the time of enzymatic degradation. Symbols are the same as in [Fig. 8](#).

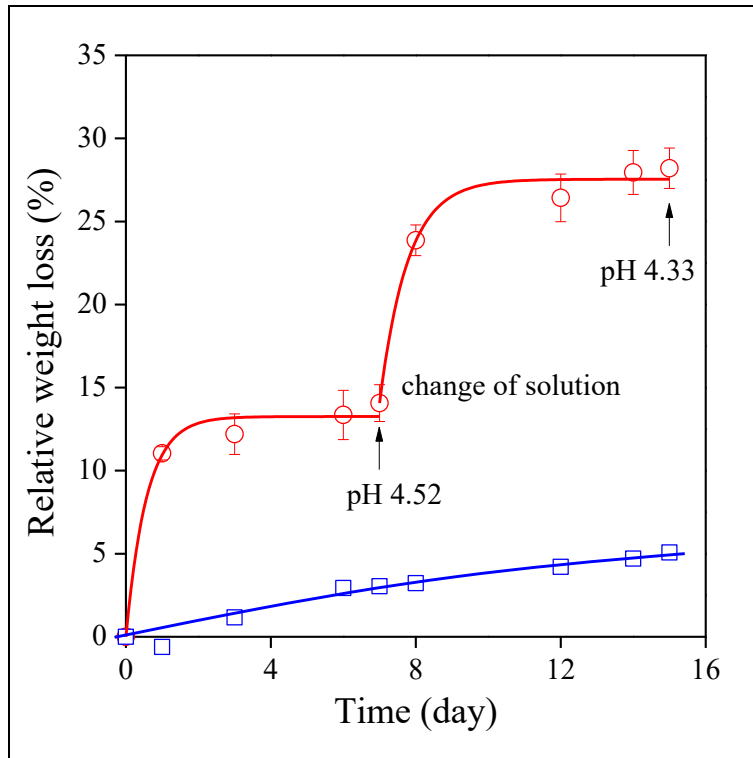
Fig. 10 pH of the degradation solution plotted against its lactic acid concentration. Non-linear correlation due to changing buffer capacity. Symbols are the same as in [Fig. 8](#).

Fig. 11 Effect of CNC content on the rate of degradation and the time constant of denaturation during the enzymatic degradation of PLA/CNC nanocomposites. Symbols: ( $\circ$ ) rate of degradation,  $v_d$ ; ( $\square$ ) time constant of denaturation,  $\tau$  (see [Eq. 1](#)).

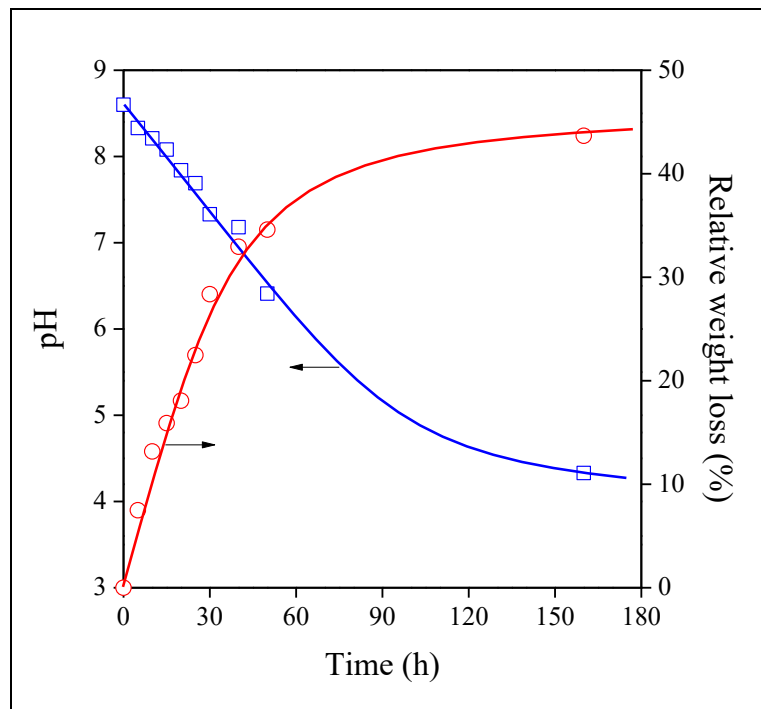
Hegyési, Fig. 1



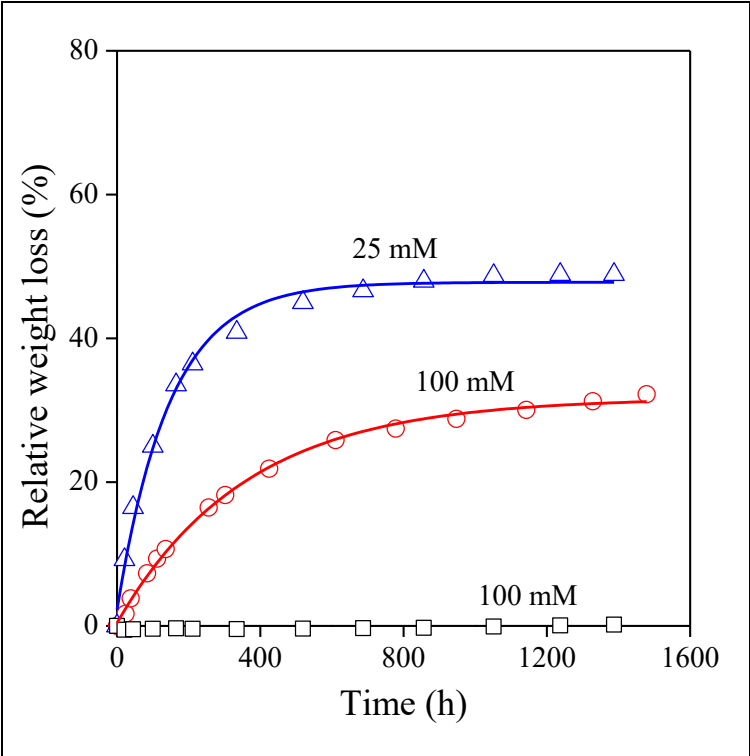
Hegyési, Fig. 2



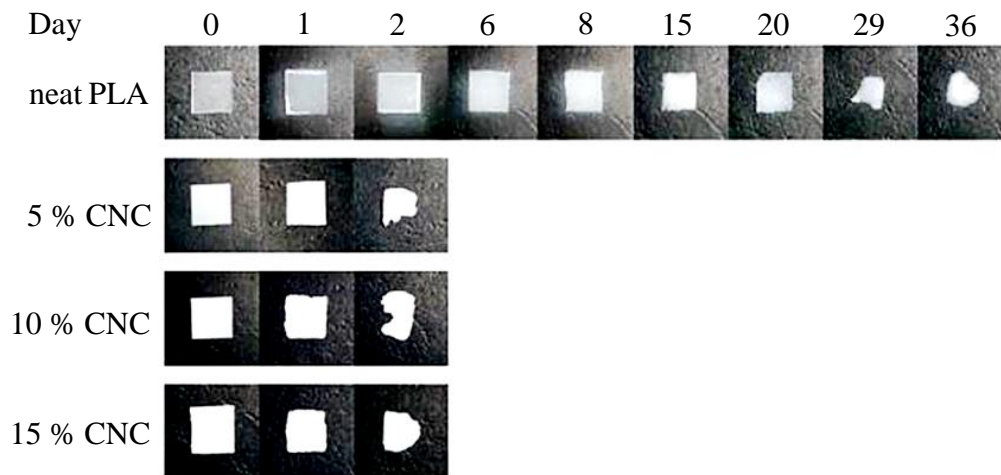
Hegyési, Fig. 3



Hegyési, Fig. 4

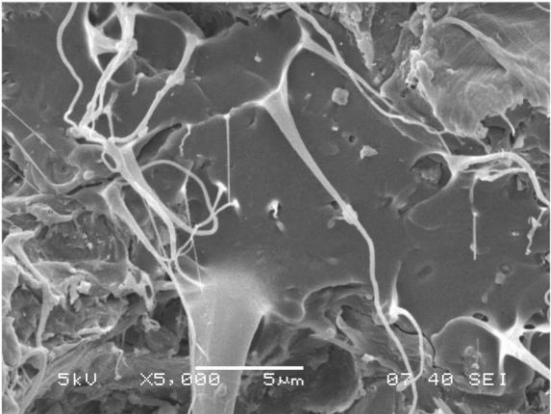


Hegyési, Fig. 5

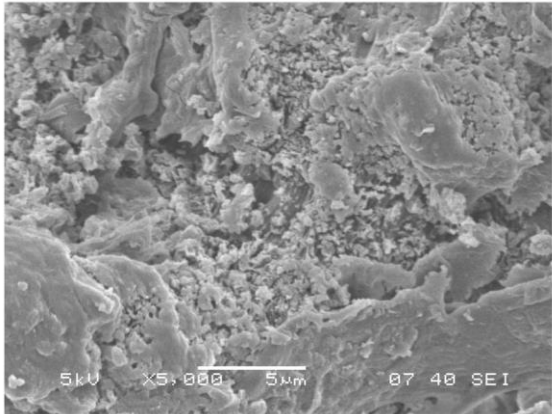


Hegyesi, Fig. 6

a)



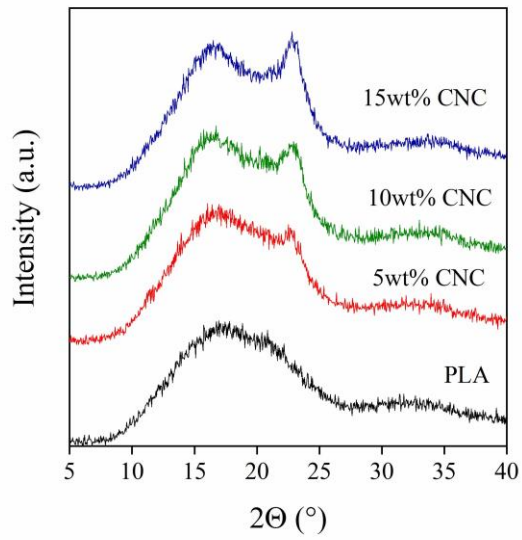
b)



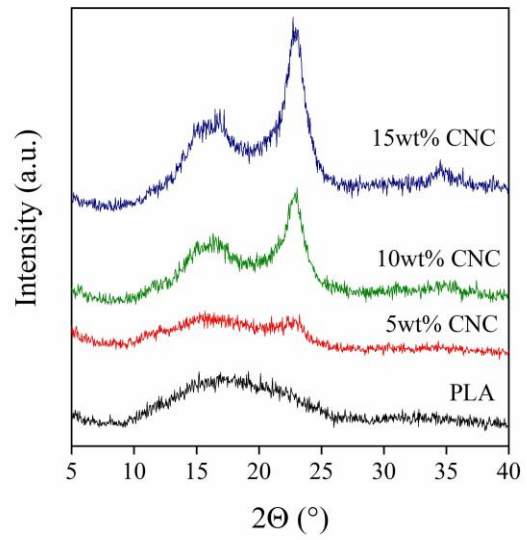


Hegyési, Fig. 7

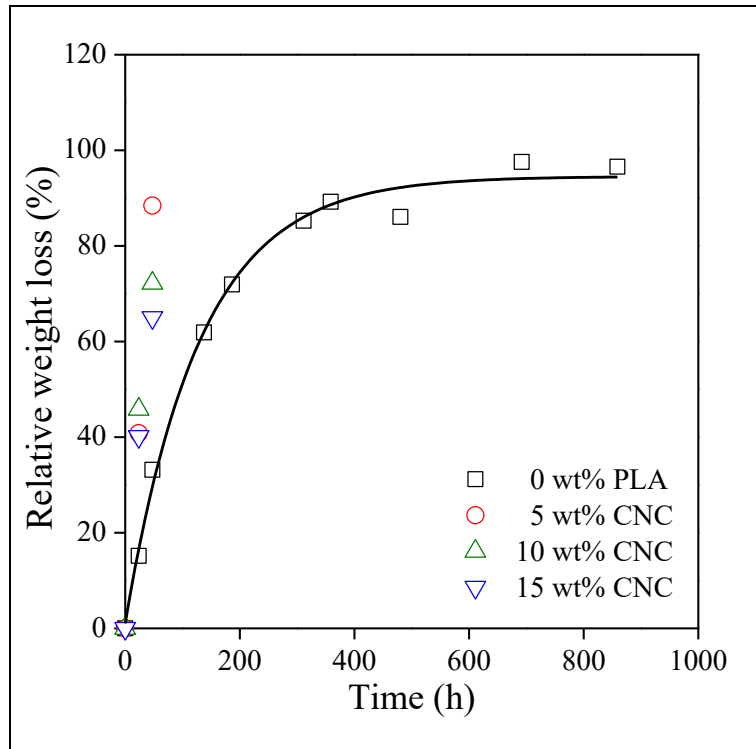
a)



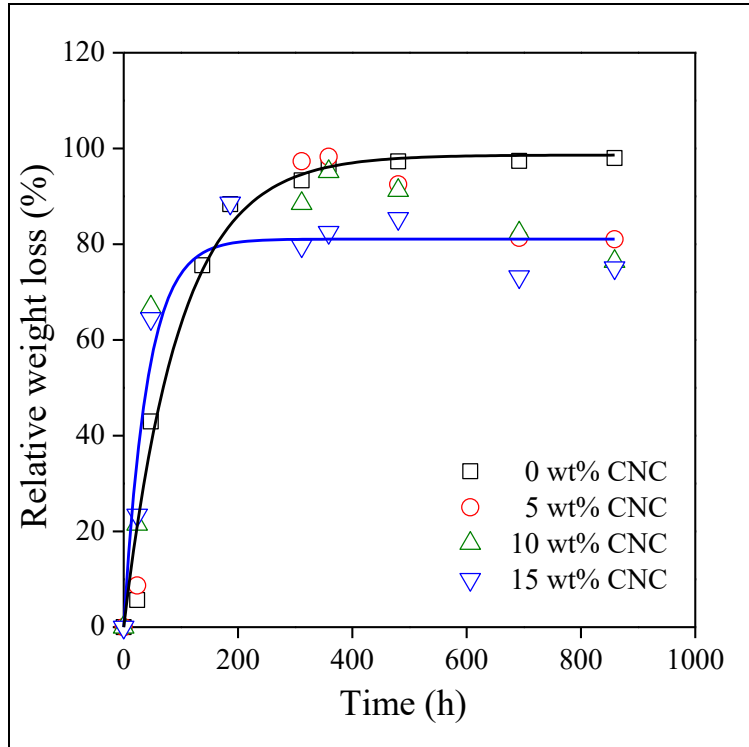
b)



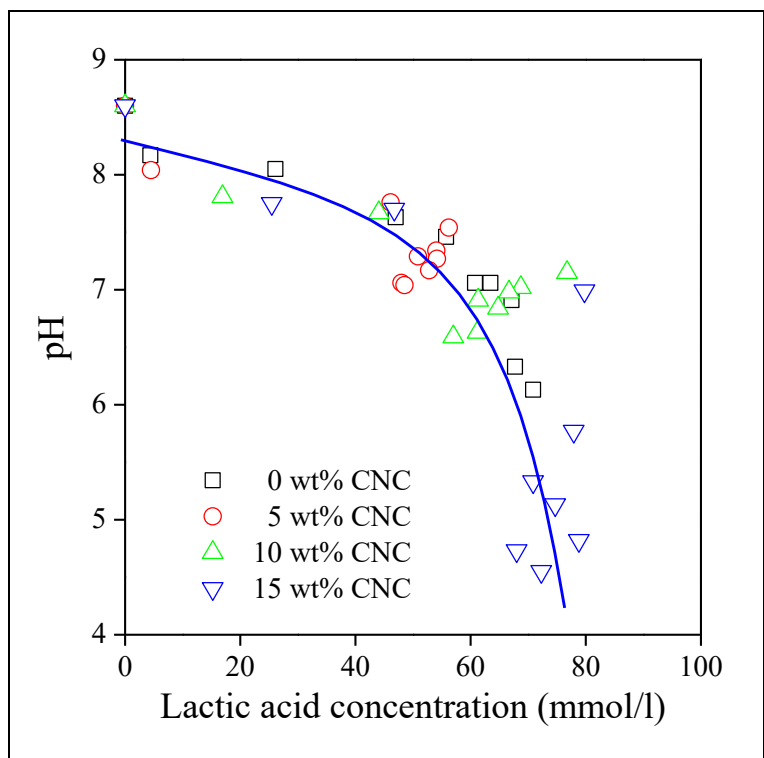
Hegyési, Fig. 8



Hegyési, Fig. 9



Hegyési, Fig. 10



Hegyési, Fig. 11

